Beyond Wigner's isobaric multiplet mass equation: Effect of charge-symmetry-breaking interaction and Coulomb polarization

J. M. Dong,[1,*] J. Z. Gu,[2] Y. H. Zhang,[1] W. Zuo,[1,3,†] L. J. Wang,[4] Yu. A. Litvinov,[5] and Y. Sun[6,7,1,‡]

[1]*Institute of Modern Physics, Chinese Academy of Sciences, Lanzhou 730000, China*
[2]*China Institute of Atomic Energy, P.O. Box 275(10), Beijing 102413, China*
[3]*School of Physics, University of Chinese Academy of Sciences, Beijing 100049, China*
[4]*Department of Physics and Astronomy, University of North Carolina, Chapel Hill, North Carolina 27516-3255, USA*
[5]*GSI Helmholtzzentrum für Schwerionenforschung, Planckstraße 1, 64291 Darmstadt, Germany*
[6]*School of Physics and Astronomy, Shanghai Jiao Tong University, Shanghai 200240, China*
[7]*Collaborative Innovation Center of IFSA, Shanghai Jiao Tong University, Shanghai 200240, China*

(Received 19 September 2018; published 25 January 2019)

The quadratic form of the isobaric multiplet mass equation (IMME), which was originally suggested by Wigner and has been generally regarded as valid, is seriously questioned by recent high-precision nuclear mass measurements. The usual resolution to this problem is to add empirically the cubic and quartic T_z terms to characterize the deviations from the IMME, but finding the origin of these terms remains an unsolved difficulty. Based on a strategy beyond Wigner's first-order perturbation, we derive explicitly the cubic and quartic T_z terms. These terms are shown to be generated by the effective charge-symmetry-breaking and charge-independence-breaking interactions in the nuclear medium combined with the Coulomb polarization effect. Calculations for the sd and lower fp shells explore a systematic emergence of the cubic T_z term, suggesting a general deviation from the original IMME. Intriguingly, the magnitude of the deviation exhibits an oscillation-like behavior with mass number, modulated by the shell effect.

DOI: 10.1103/PhysRevC.99.014319

I. INTRODUCTION

Shortly after the discovery of the neutron, Heisenberg introduced isospin to describe different charge states of the nucleon [1]. In this concept, the proton (p) and neutron (n) are treated as an isospin $T = 1/2$ doublet distinguished by different projections $T_z(p) = -1/2$ and $T_z(n) = +1/2$. As one of the most important predictions in nuclear physics, the isobaric multiplet mass equation (IMME) proposed later by Wigner [2,3] suggests that the mass excesses ME(A, T, T_z) of the nuclei belonging to an isospin multiplet of mass number A and total isospin T follow a simple quadratic equation,

$$\mathrm{ME}(A, T, T_z) = a + bT_z + cT_z^2, \tag{1}$$

where $T_z = (N - Z)/2$ is the isospin projection, and the parameters a, b, and c are constants for a given multiplet. The elegant IMME, though derived by using the first-order perturbation approximation, has been widely employed to predict the unknown masses of unstable neutron-deficient nuclei.

Since its establishment, the IMME is believed to be generally valid [4]. With recent advances in radioactive beam facilities, a wealth of exotic masses with increasing precision became available [5]. Unexpectedly large discrepancies between the measured masses and the ones given by the quadratic form of the IMME were observed [6–8]. This calls for an addition of a cubic term dT_z^3 or even a quartic term eT_z^4 to Eq. (1) [9–11]. The origin of these higher-order terms, which clearly lies beyond the original IMME of Eq. (1), requires explanation.

Various mechanisms have been proposed to explain the deviations found in individual cases, including the isospin mixing, the high-order Coulomb effect, and the charge-dependent nucleon-nucleon interaction [12–15]. However, to date there is no consensus as to the origin of the observed large dT_z^3 terms. In current shell-model calculations, isospin-nonconversing (INC) interactions are determined through fitting to available experimental data [16–20], which are, however, insufficient to explain the experimental dT_z^3 terms.

In a recent work [21], we have laid out a theoretical framework which considers the contributions of the charge-symmetry-breaking (CSB) and charge-independence-breaking (CIB) components in the nuclear medium to the effective nucleon-nucleon force. We have found that such effective INC interactions are density dependent, and thus can no longer be expressed as irreducible tensors as was done by Wigner [2,3]. This leads us to propose a generalized IMME (GIMME) [21] to study the Nolen-Schiffer anomaly, which is expressed as [21]

$$\mathrm{ME}(A, T, T_z) = a + \left(b_c + \Delta_{\mathrm{nH}} + 2a_{\mathrm{sym},1}^{(\mathrm{CSB})}(A, T_z)\right)T_z + \left(c_c + \frac{4}{A}a_{\mathrm{sym},2}^{(\mathrm{CIB})}(A, T_z)\right)T_z^2, \tag{2}$$

*dongjm07@impcas.ac.cn
†zuowei@impcas.ac.cn
‡sunyang@sjtu.edu.cn

where $\Delta_{\rm nH} = 0.782$ MeV is the neutron-hydrogen mass difference. In Eq. (2), the two anticipated isospin-symmetry breaking sources, the Coulomb and the nuclear interactions, are clearly separated. The T_z-independent b_c and c_c coefficients are produced solely by the Coulomb interaction, whereas the first (second)-order symmetry energy $a^{(\rm CSB)}_{\rm sym,1}$ ($a^{(\rm CIB)}_{\rm sym,2}$) originates from the CSB (CIB) interaction in the nuclear medium [21].

In this paper we apply the GIMME [21] to explore the physics beyond the first-order perturbation in the IMME. We show that the appearance of the high-order T_z terms is a more general phenomenon, and that the degree of the deviation to Eq. (1), measured by the coefficient of the T_z^3 term, is totally governed by shell effects with a remarkable A dependence.

II. $T = 3/2$ ISOBARIC QUARTETS

Within the first-order perturbation calculation, $|\alpha T T_z\rangle$ is assumed to be an eigenstate of the charge-independent Hamiltonian H_0, with α for all additional quantum numbers to label this state. The energy produced by the CSB and CIB interactions is given by $\langle \alpha T T_z|H_{\rm CSB+CIB}|\alpha T T_z\rangle = 2a^{(\rm CSB)}_{\rm sym,1}(A,T_z)T_z + \frac{4}{A}a^{(\rm CIB)}_{\rm sym,2}(A,T_z)T_z^2$ in the absence of the Coulomb force [21]. In this case, the $a^{(\rm CSB)}_{\rm sym,1}(A,T_z)$ [and also $a^{(\rm CIB)}_{\rm sym,2}(A,T_z)$] is identical for all members of an isobaric multiplet, as seen in the Appendix. Thus, the GIMME is reduced to the quadratic form of the IMME. However, if we go beyond the first-order perturbation to calculate $\langle \alpha T_z|H_{\rm CSB+CIB}|\alpha T_z\rangle$ with inclusion of the Coulomb polarization effect, $a^{(\rm CSB)}_{\rm sym,1}(A,T_z)$ [and also $a^{(\rm CIB)}_{\rm sym,2}(A,T_z)$] is no longer a constant for a given isobaric multiplet. One may formally expand them to be $a^{(\rm CSB)}_{\rm sym,1}(A,T_z)T_z = a_1 + b_1T_z + c_1T_z^2 + d_1T_z^3$ and $a^{(\rm CIB)}_{\rm sym,2}(A,T_z)T_z^2 = a_2 + b_2T_z + c_2T_z^2 + d_2T_z^3$ for the $T = 3/2$ quartets. Equation (2) can then be rearranged as

$$\mathrm{ME}(A,T,T_z) = a + bT_z + cT_z^2 + dT_z^3, \tag{3}$$

where the d coefficient is explicitly expressed as

$$d = -\frac{8\pi}{9}\int_0^\infty r^2 S_1^{(\rm CSB)}(\rho)(\delta\rho_{3/2} - \delta\rho_{-3/2})dr - \frac{8\pi}{9}\int_0^\infty \frac{r^2}{\rho(r)} S_2^{(\rm CIB)}(\rho)\left(\delta\rho_{3/2}^2 - \delta\rho_{-3/2}^2\right)dr. \tag{4}$$

In Eq. (4), $\delta\rho_{T_z} = [\rho_n(r) - \rho_p(r)]^{\rm core}_{T_z}$ is the neutron- and proton-density difference in the core of the nucleus with T_z. For $T = T_z$ ($-T_z$) nuclei, where there are $|N - Z|$ excess neutrons (protons), we call the remaining nucleons (with an equal number of protons and neutrons) the "core" in the discussion. The terms $S_1^{(\rm CSB)}$ and $S_2^{(\rm CIB)}$ in Eq. (4) are density-dependent symmetry energies characterizing the INC interactions, defined as

$$S_1^{(\rm CSB)}(\rho) = \left.\frac{\partial E^{(\rm CSB)}(\rho,\beta)}{\partial\beta}\right|_{\beta=0}, \tag{5}$$

$$S_2^{(\rm CIB)}(\rho) = \left.\frac{1}{2}\frac{\partial^2 E^{(\rm CIB)}(\rho,\beta)}{\partial\beta^2}\right|_{\beta=0}. \tag{6}$$

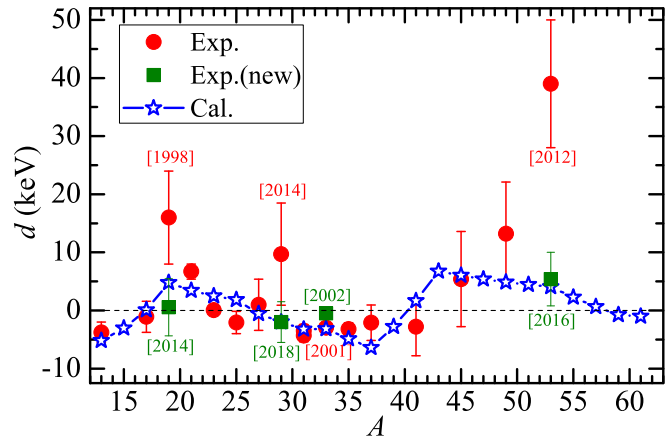

FIG. 1. d values for $T = 3/2$ quartets calculated with Eq. (4). The presented experimental data are from Refs. [11,23] for $A = 19$, [8] for 21, [11,24] for 29, [25,26] for 31, [27,28] for 33, [29] for 35, [30] for 37, [7] for $41 - 49$, [7,31] for 53, and the remaining data are taken from Ref. [11]. The numbers in brackets refer to the years of publication.

The above results are achieved based on the microscopic Brueckner-Hartree-Fock approach with the AV18 (together with AV14) interaction [21], in which $E^{(\rm CSB)}$ ($E^{(\rm CIB)}$) is the energy associated with the CSB (CIB) interaction. The CIB interaction contribution is about one order of magnitude smaller than that of the CSB interaction. From Eq. (4), the nonzero d originates primarily from the first-order symmetry energy difference between the $T_z = 3/2$ core and $T_z = -3/2$ core. The nucleonic density distributions inside the nucleus are calculated within a Skyrme energy-density functional approach. Detailed derivations of Eqs. (3) and (4) are given in the Appendix. We note that the dT_z^3 term is usually added empirically to account for deviations from the quadratic form of the IMME, but here it is derived microscopically. The occurrence of the nonzero d coefficient is due to a combined effect of the CSB interaction in the nuclear medium together with the treatment of the beyond-first-order perturbation calculation (i.e., by including the core polarization induced by the Coulomb force). Both of them are indispensable. We thus conclude that although the high-order Coulomb contribution to the d value is generally believed to be small [22], it is necessarily included because without it, as we discussed in detail before Eq. (3), the d term would not appear.

In Fig. 1, we show the d values calculated with Eq. (4) for $T = 3/2$ isobaric quartets. The SLy4 interaction [32] that satisfies specific constraints defined in our previous work [33] is employed to compute the nucleonic density distributions. Remarkably, the results for the d coefficients exhibit a clear A dependence. It is striking that, across the sd and lower fp shells, the d values show an oscillation-like behavior with a minimum ~ -6 keV and maximum ~ 7 keV. The crossing points of the curve with the $d = 0$ line correspond to the multiplets involving the magic numbers 8, 20, and 28, implying the underlying shell effect.

Experimental data seem to support the above prediction. In Fig. 1, we also plot the experimentally extracted

d values for the isobaric quartets from the measured mass excesses via $d = [\mathrm{ME}(T_z = 3/2) - \mathrm{ME}(T_z = -3/2) - 3\,\mathrm{ME}(T_z = 1/2) + 3\,\mathrm{ME}(T_z = -1/2)]/6$. These experimental d values follow the predicted pattern well.

As one can see from Fig. 1, the experimental d values for $A = 31$ [25,26], 33 [27,28], and 35 [29] multiplets have small uncertainties. Our calculations reproduce these data. With the new mass of ^{29}S measured recently with the isochronous mass spectrometry technique in the experimental cooler storage ring (CSRe) at the Heavy Ion Research Facility in Lanzhou [24], the IMME is shown to be revalidated for $A = 29$, which is supported by our calculation. However, the validity of the IMME represents only special cases of our general conclusion.

For the $T_z = 3/2$ isobaric quartets, the first test in the fp shell with $A = 45$, 49, and 53 indicated systematical deviations from the IMME [7]. Calculations based on two INC Hamiltonians, the $f_{7/2}$ model space [34] and the full pf model space with the GPFX1A interaction [35,36] plus the Ormand-Brown INC Hamiltonian [16], could not reproduce the experimental data [7]. Our calculated d values for $A = 41$, 45, and 49 shown in Fig. 1 agree qualitatively with experiment. For $A = 53$, Ref. [7] initially reported a very large $d = 39(11)$ keV. With a later remeasurement of the IAS of ^{53}Co [31], it was reduced and agrees now well with our prediction (see Fig. 1). From our calculations, significant d values are expected in the pf shell. Precision mass measurements of the relevant nuclei are required. Especially interesting would be the confirmation of the maximum d value at $A = 43$, for which the identification and mass determination of the $T = 3/2$ IAS in ^{43}Ti are needed.

The $A = 21$ multiplet has been taken in Ref. [8] as an example to show violations of the IMME in the sd shell nuclei. The universal sd USDA and USDB isospin-conserving Hamiltonians supplemented with an INC part yield too small d values ($d = -0.3$ keV (USDA) and 0.3 keV (USDB) for the $A = 21$, $J^\pi = 5/2^+$ quartet [8]). The valence-space calculations based on the low-momentum two-nucleon and three-nucleon forces derived from the chiral effective field theory [37] give $d = -38$ keV for the $A = 21$ quartet [8], which disagrees with the experimental value 6.7(13) keV. Our result $d = 3.4$ keV is close to the experimental data.

We stress that the occurrence of nonzero d's, which marks deviations from the original IMME, is fundamental. The variation of the d coefficient is driven by the shell effect. We find that once the excess neutrons in the $T_z = 3/2$ of a multiplet fill a level below (above) a large shell gap, as schematically illustrated in the left (right) panel of Fig. 2(a), the smallest (largest) d value appears (see Fig. 1). For instance, the $T_z = T$ member of the $A = 37$ ($A = 43$) multiplet, ^{37}Cl (^{43}Ca), has three excess neutrons filling below (above) the $N = 20$ shell gap. When A changes from 37 to 43, the excess neutrons (protons) for $T_z = 3/2$ ($T_z = -3/2$) member gradually occupy the upper $1f_{7/2}$ orbit. The neutrons (protons) in the core tend to be more loosely (tightly) bound if they and the excess neutrons (protons) fill the same (different) orbit(s), leading to the A-dependent differences in neutron (proton) density of the core. As seen in Fig. 2(b), when A changes from 37 to 43, $\delta\rho_{3/2} - \delta\rho_{-3/2} = [\rho_n^{\mathrm{core}}(r) - \rho_p(r)]_{T_z=3/2} + [\rho_p^{\mathrm{core}}(r) - \rho_n(r)]_{T_z=-3/2}$ increases significantly, particularly in the region of $r = 1$–3 fm. This shell effect is brought into the d coefficient via the integral in Eq. (4). In the $T = 3/2$ multiplets, the excess neutrons (protons) in the $T_z = 3/2$ ($T_z = -3/2$) nuclei occupy a level above the $1p_{1/2} - 1d_{5/2}$ or $1d_{3/2} - 1f_{7/2}$ shell gap for the $A = 21$ or $A = 45$–53 quartets, respectively, leading to a relatively large violation of the IMME. This mechanism holds also true for the strong breakdown of the $A = 9$ quartet since the excess neutrons (protons) in the $T_z = 3/2$ ($T_z = -3/2$) nuclei occupy a level above the $1s_{1/2} - 1p_{3/2}$ shell gap. However, the $A = 9$ quartet is excluded from Fig. 1 for discussion because, generally, the Skyrme functional does not quantitatively apply to such light nuclei. We conclude that the magnitude of the d coefficient, which measures the degree of deviation from the original IMME, depends on the shell filling.

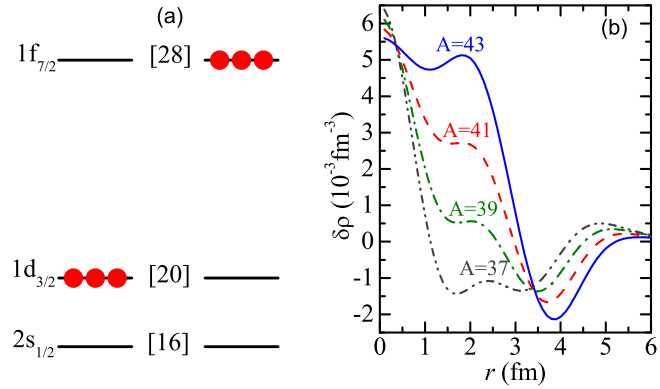

FIG. 2. (a) Schematic illustration highlighting the filling pattern of excess neutrons for the $T_z = T$ nucleus. (b) The core density difference $\delta\rho_{3/2} - \delta\rho_{-3/2}$ for $T = 3/2$ isobaric quartets. The case for $A = 37$ ($A = 43$) corresponds to the left (right) shell-filling pattern in (a).

As shown in Fig. 1, we predict a local maximum of d for the $A = 19$ quartet. The existing experimental measurements are divergent for the excitation energy of the IAS in ^{19}Ne [11,23], leading to completely different conclusions regarding the IMME. An experimental confirmation of this energy is necessary.

III. $T = 2$ ISOBARIC QUINTETS

With the similar derivation for $T = 3/2$ quartets, the GIMME of Eq. (2) is rewritten for $T = 2$ quintets as

$$\mathrm{ME}(A, T, T_z) = a + bT_z + cT_z^2 + dT_z^3 + eT_z^4, \quad (7)$$

with the d and e coefficients given as

$$d = -\frac{\pi}{4}\int_0^\infty r^2 S_1^{(\mathrm{CSB})}(\rho)(\delta\rho_2 - \delta\rho_{-2})dr - \frac{\pi}{4}\int_0^\infty \frac{r^2}{\rho(r)} S_2^{(\mathrm{CIB})}(\rho)\left(\delta\rho_2^2 - \delta\rho_{-2}^2\right)dr, \quad (8)$$

$$e = -\frac{\pi}{64}\int_0^\infty dr\,\frac{r^2}{\rho(r)} S_2^{(\mathrm{CIB})}(\rho)(\delta\rho_2 - \delta\rho_{-2}) \times \left[11(\delta\rho_2 - \delta\rho_{-2}) + 8\left(\rho_n^{\mathrm{exc}}|_{T_z=2} + \rho_p^{\mathrm{exc}}|_{T_z=-2}\right)\right], \quad (9)$$

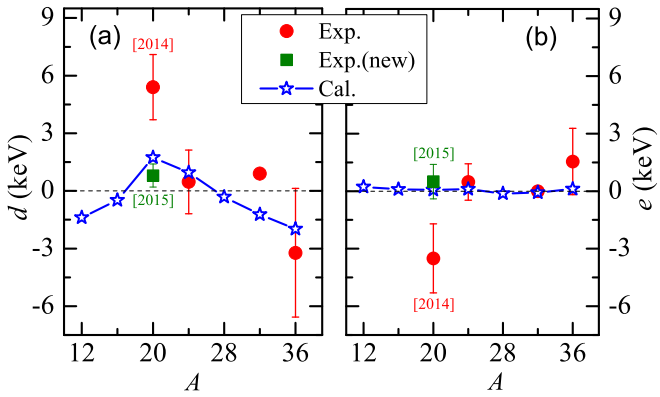

FIG. 3. d and e values for $T = 2$ quintets calculated with Eqs. (8) and (9). The presented experimental data are taken from Refs. [8,38] for $A = 20$, and the remaining data are from Ref. [11]. The numbers in brackets refer to the years of publication.

where $\rho_n^{\rm exc}|_{T_z=2}$ ($\rho_p^{\rm exc}|_{T_z=-2}$) is the density of the $|N-Z|$ excess neutrons (protons) in the $T_z = T$ ($T_z = -T$) nucleus. The e coefficient just originates from the CIB interaction, and the detailed derivation is presented in the Appendix.

In Fig. 3, we compare the calculated d and e values for $T = 2$ quintets with the available experimental data. The calculations suggest that the d values are overall small, and the magnitude does not exceed 2 keV. The calculated d values for $A = 12$–36 in Fig. 3(a) show a similar pattern as the one for $T = 3/2$ quartets with a maximum at $A = 20$. The occurrence of this variation shares the same physical origin as that in the $T = 3/2$ quartets, namely the excess neutrons in the $T_z = T = 2$ member occupy a level above the $1p_{1/2}-1d_{5/2}$ shell gap, resulting in a relatively larger d value as compared with those of its neighbors.

In 2014, a significant violation of the IMME for the $A = 20$ quintet was reported [8]. However, with a later measurement of the excitation energy of the lowest $T = 2$ state in ^{20}Na, the IMME was revalidated [38]. Our calculated value of $d = 1.7$ keV is in agreement with the later experimental measurement [see Fig. 3(a)]. The calculation presented in Ref. [8] deviates substantially from both measurements.

The data point for $A = 32$ shows a deviation from our calculated value. The studies of this quintet were carried out by several collaborations [39–43], and some of the measured data are controversial [43]. We note that both the experimental and our predicted values are small. The calculated and experimental e values are compatible with zero, and they are in agreement with each other.

IV. SUMMARY

Based on our recently proposed GIMME [21], we have established an isobaric multiplet mass equation that includes high-order terms within a new strategy beyond the first-order perturbation approximation. The explicit expression of d (and also e) coefficient which quantifies the deviation of the quadratic form of the original IMME has been derived. The emergence of the nonzero cubic T_z term, and hence the violation of the quadratic IMME, have basic roots. We have found that the charge-symmetry-breaking interaction in the nuclear medium, characterized in our theory by the first-order symmetry energy, combined with the core polarization effect primarily induced by the Coulomb force, are responsible for the breakdown of the quadratic IMME. The effective charge-symmetry-breaking and charge-independence-breaking interactions were extracted by employing an *ab initio* method, i.e., the Brueckner theory with bare AV18 and AV14 interactions without any phenomenological adjustments. Remarkably, we found that the calculated d values for quartets and quintets follow an oscillation-like behavior throughout the sd- and lower fp-shell regions as a consequence of the shell effect, and the experimental d values extracted from the measured masses agree with the oscillation pattern qualitatively. If all excess neutrons in the $T_z = T$ nucleus of a multiplet fill a level above a large shell gap, the breakdown of the quadratic IMME tends to be strong. Therefore, it is straightforward to predict the nuclei where the strong deviations from the original IMME are expected, which is essential for guiding future experimental efforts.

ACKNOWLEDGMENTS

This work was supported by the National Natural Science Foundation of China under Grants No. 11775276, No. 11435014, No. 11405223, No. 11675265, and No. 11575112, by the 973 Program of China under Grants No. 2013CB834401 and No. 2013CB834405, by the National Key Program for S&T Research and Development (No. 2016YFA0400501, No. 2016YFA0400502), by the Youth Innovation Promotion Association of Chinese Academy of Sciences, by the Helmholtz-CAS Joint Research Group HCJRG-108, and by the European Research Council (ERC) under the European Union's Horizon 2020 research and innovation program (Grant agreement No. 682841 "ASTRUm"). Y.H.Z. acknowledges support by the ExtreMe Matter Institute EMMI at the GSI Helmholtzzentrum für Schwerionenforschung, Darmstadt, Germany.

APPENDIX

The 1st-order symmetry energy $a_{\rm sym,1}^{\rm (CSB)}(A, T_z)$ and the 2nd-order one $a_{\rm sym,2}^{\rm (CIB)}(A, T_z)$ for finite nuclei in Eq. (2) originate from the CSB and CIB interactions in nuclear medium, respectively, which can be expressed as [21]

$$a_{\rm sym,1}^{\rm (CSB)}(A, T_z) = \frac{1}{IA}\int_0^\infty 4\pi r^2 \rho(r) S_1^{\rm (CSB)}(\rho)\beta(r)dr, \quad \text{(A1)}$$

$$a_{\rm sym,2}^{\rm (CIB)}(A, T_z) = \frac{1}{I^2 A}\int_0^\infty 4\pi r^2 \rho(r) S_2^{\rm (CIB)}(\rho)\beta^2(r)dr, \quad \text{(A2)}$$

where $I = (N-Z)/A = 2T_z/A$ is the isospin asymmetry of a given nucleus. $\beta(r) = (\rho_n(r) - \rho_p(r))/\rho(r)$ is the local isospin asymmetry in which $\rho_p(r)$ and $\rho_n(r)$ are the proton and neutron density distributions inside the nucleus. Here the

symmetry energy coefficient is called simply as the symmetry energy. The spherical-nuclei approximation is employed to achieve a concise result. To achieve the $a^{(\mathrm{CSB})}_{\mathrm{sym},1}(A,T_z)$ and $a^{(\mathrm{CIB})}_{\mathrm{sym},2}(A,T_z)$, we should gain the nucleonic density distributions ρ_n and ρ_p of an isobaric analog state (IAS) whose T is larger than $|T_z|$.

We assume $|\alpha T T_z\rangle$ is the eigenstate of the charge-independent Hamiltonian H_0, with α for all additional quantum numbers to label this state. In the first-order perturbation, the energy produced by the CSB and CIB interactions is given by $\langle\alpha T T_z|H_{\mathrm{CSB+CIB}}|\alpha T T_z\rangle = 2a^{(\mathrm{CSB})}_{\mathrm{sym},1}(A,T_z)T_z + \frac{4}{A}a^{(\mathrm{CIB})}_{\mathrm{sym},2}(A,T_z)T_z^2$ in the absence of Coulomb force [21]. In this case, the wave function of the IAS (with $T_z = T-1$) with $N-1$ neutrons and $Z+1$ protons ($N>Z$) is obtained with $|\mathrm{IAS}\rangle = |T, T_z = T-1\rangle = \frac{1}{\sqrt{2T}}T_-|0\rangle$ [44] rigidly, where $T_- = \sum t_-(j)$ is the isospin lowering operator, j ∈ excess neutron orbits in $|0\rangle$. $|0\rangle$ is the ground state of the parent nucleus with N neutrons and Z protons belonging to a multiplet with $T = T_z$. Thus, $(\rho_n+\rho_p)_{\mathrm{IAS}} = (\rho_n+\rho_p)_{\mathrm{parent}}$ and $(\rho_n-\rho_p)_{\mathrm{IAS}} = (1-\frac{1}{T})(\rho_n-\rho_p)_{\mathrm{parent}}$ are obtained. The same situation also applies to the IAS with $T_z = -(T-1)$. Accordingly, the $a^{(\mathrm{CSB})}_{\mathrm{sym},1}(A,T_z)$ (and also $a^{(\mathrm{CIB})}_{\mathrm{sym},2}(A,T_z)$) is identical for all members of an isobaric multiplet. Therefore, they can be merged into the b_c and c_c, respectively. Namely, the GIMME is reduced to the quadratic form of the IMME, and hence the IMME is not breakdown.

Here we treat this energy produced by CSB and CIB interactions beyond the first-order perturbation approximation, i.e., calculate the $\langle\alpha T_z|H_{\mathrm{CSB+CIB}}|\alpha T_z\rangle$ instead of $\langle\alpha T T_z|H_{\mathrm{CSB+CIB}}|\alpha T T_z\rangle$, with the inclusion of Coulomb interaction. Accordingly, the $a^{(\mathrm{CSB})}_{\mathrm{sym},1}(A,T_z)$ (and also $a^{(\mathrm{CIB})}_{\mathrm{sym},2}(A,T_z)$) is no longer a constant for a given isobaric multiplet. Yet, we can expand them as $a^{(\mathrm{CSB})}_{\mathrm{sym},1}(A,T_z)T_z = a_1 + b_1T_z + c_1T_z^2 + d_1T_z^3$ and $a^{(\mathrm{CIB})}_{\mathrm{sym},2}(A,T_z)T_z^2 = a_2 + b_2T_z + c_2T_z^2 + d_2T_z^3$ for $T = 3/2$ isobaric quartets, and thus Eq. (2) is written as

$$\begin{aligned}\mathrm{ME}(A,T,T_z) &= a + (b_c+\Delta_{\mathrm{nH}})T_z + 2\left(a_1 + b_1T_z + c_1T_z^2 + d_1T_z^3\right) + c_cT_z^2 + \frac{4}{A}\left(a_2 + b_2T_z + c_2T_z^2 + d_2T_z^3\right),\\ &= \left(a + 2a_1 + \frac{4a_2}{A}\right) + \left(b_c + \Delta_{\mathrm{nH}} + 2b_1 + \frac{4b_2}{A}\right)T_z + \left(c_c + 2c_1 + \frac{4c_2}{A}\right)T_z^2 + \left(2d_1 + \frac{4d_2}{A}\right)T_z^3. \quad \text{(A3)}\end{aligned}$$

Therefore, if we introduce a new a coefficient to replace the $a + 2a_1 + \frac{4a_2}{A}$, and define the b, c, d coefficients by

$$b = b_c + \Delta_{\mathrm{nH}} + 2b_1 + \frac{4b_2}{A}, \quad c = c_c + 2c_1 + \frac{4c_2}{A}, \quad d = 2d_1 + \frac{4d_2}{A} \quad \text{(A4)}$$

then the GIMME for quartets is rewritten as

$$\mathrm{ME}(A,T,T_z) = a + bT_z + cT_z^2 + dT_z^3. \quad \text{(A5)}$$

The central task is to calculate the d coefficient. It should be stressed that, because of the core polarization induced by the Coulomb force, the state of the $T_-|0\rangle/\sqrt{2T}$ is not the exact description of the physical analog state ($T_z = T-1$). The excess neutron density $\rho^{\mathrm{exc.}}_{n,\mathrm{parent}}$, instead of $\rho_n - \rho_p$ should be used in the transition density, as discussed in Ref. [45]. Therefore, one obtains

$$(\rho_n-\rho_p)_{T_z=T-1} = \left(1-\frac{1}{T}\right)(\rho_n-\rho_p)_{T_z=T} + \frac{1}{T}\delta\rho_{T_z=T}, \quad \text{(A6)}$$

where $\delta\rho(r) = \rho_n^{\mathrm{core}}(r) - \rho_p(r)$ is the neutron- and proton-density difference in the core (with an equal number of protons and neutrons) in the $T_z = T$ nucleus. The same situation also applies to the IAS with $T_z = -(T-1)$. In order to improve the accuracy, we use the

$$(\rho_n-\rho_p)_{T_z=T-1} = \left(1-\frac{1}{T}\right)(\rho_n-\rho_p)_{T_z=T} + \frac{1}{2T}(\delta\rho_{T_z=T} + \delta\rho_{T_z=T-1}). \quad \text{(A7)}$$

In Fig. 4, we give two examples for $T = 1/2$ doublet to show the validity of such a treatment. Eq. (A7)

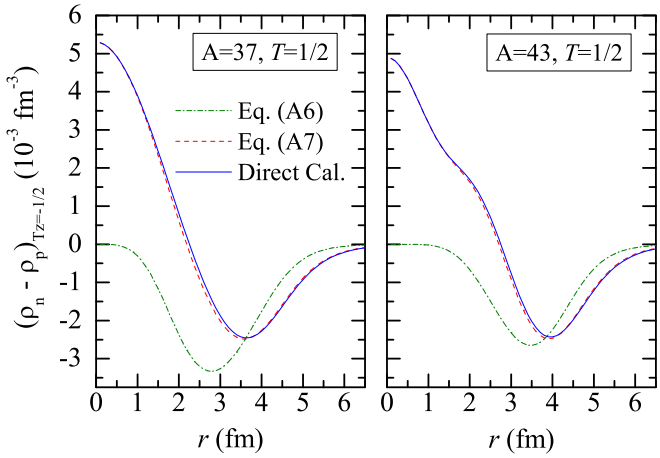

FIG. 4. The density difference between the neutron and proton, i.e., $\rho_n - \rho_p$, for $A = 37$ and $A = 43$ isobaric doublets as examples. The Eqs. (A6) and (A7) are employed to calculate the $\rho_n - \rho_p$ of $T_z = -1/2$ nuclei in the framework of the Skyrme-Hartree-Fock method, and compared with the direct calculation with the Skyrme-Hartree-Fock method.

works rather well, and is much better than Eq. (A6). In a word, for the $T = 3/2$ isobaric quartets, the density difference $\rho_n - \rho_p$ is summarized as

$$\rho_n - \rho_p = \begin{cases} (\rho_n - \rho_p)_{T_z=3/2}, & T_z = \frac{3}{2} \\ \frac{1}{3}(\rho_n - \rho_p)_{T_z=3/2} + \frac{1}{3}(\delta\rho_{3/2} + \delta\rho_{1/2}), & T_z = \frac{1}{2} \\ \frac{1}{3}(\rho_n - \rho_p)_{T_z=-3/2} + \frac{1}{3}(\delta\rho_{-3/2} + \delta\rho_{-1/2}), & T_z = -\frac{1}{2} \\ (\rho_n - \rho_p)_{T_z=-3/2}, & T_z = -\frac{3}{2} \end{cases} \tag{A8}$$

with $\delta\rho_{_{T_z}} = [\rho_n^{\rm core}(r) - \rho_p(r)]_{_{T_z}} = [\rho_n(r) - \rho_p(r)]_{T_z}^{\rm core}$.

We assume that $\delta\rho_{3/2}, \delta\rho_{1/2}, \delta\rho_{-1/2}, \delta\rho_{-3/2}$ are equidistant since the proton number is equidistantly increasing from $T_z = 3/2$ to $T_z = -3/2$ nuclei, and hence $(\delta\rho_{3/2} - \delta\rho_{-3/2}) = 3(\delta\rho_{1/2} - \delta\rho_{-1/2})$. Since we expand the first-order and the second-order symmetry energy produced by the CSB and CIB interactions as $a_{\rm sym,1}^{\rm (CSB)}(A, T_z)T_z = a_1 + b_1T_z + c_1T_z^2 + d_1T_z^3$ and $a_{\rm sym,2}^{\rm (CIB)}(A, T_z)T_z^2 = a_2 + b_2T_z + c_2T_z^2 + d_2T_z^3$, the d_1 and d_2 are given as

$$\begin{aligned}
2d_1 &= \frac{1}{2}\left[a_{\rm sym,1}^{\rm (CSB)}\left(A, \frac{3}{2}\right) + a_{\rm sym,1}^{\rm (CSB)}\left(A, -\frac{3}{2}\right) - a_{\rm sym,1}^{\rm (CSB)}\left(A, \frac{1}{2}\right) - a_{\rm sym,1}^{\rm (CSB)}\left(A, -\frac{1}{2}\right)\right] \\
&= \frac{1}{2}\frac{1}{3}\int_0^\infty 4\pi r^2 S_1^{\rm (CSB)}(\rho)(\rho_n - \rho_p)_{T_z=3/2}dr - \frac{1}{2}\frac{1}{3}\int_0^\infty 4\pi r^2 S_1^{\rm (CSB)}(\rho)(\rho_n - \rho_p)_{T_z=-3/2}dr \\
&\quad - \frac{1}{2}\int_0^\infty 4\pi r^2 S_1^{\rm (CSB)}(\rho)\left[\frac{1}{3}(\rho_n - \rho_p)_{T_z=3/2} + \frac{1}{3}(\delta\rho_{3/2} + \delta\rho_{1/2})\right]dr \\
&\quad + \frac{1}{2}\int_0^\infty 4\pi r^2 S_1^{\rm (CSB)}(\rho)\left[\frac{1}{3}(\rho_n - \rho_p)_{T_z=-3/2} + \frac{1}{3}(\delta\rho_{-3/2} + \delta\rho_{-1/2})\right]dr \\
&= \frac{1}{6}\int_0^\infty dr 4\pi r^2 S_1^{\rm (CSB)}(\rho)\cdot\left\{(\rho_n - \rho_p)_{T_z=3/2} - (\rho_n - \rho_p)_{T_z=-3/2} - 3\left[\frac{1}{3}(\rho_n - \rho_p)_{T_z=3/2} + \frac{1}{3}(\delta\rho_{3/2} + \delta\rho_{1/2})\right]\right. \\
&\quad \left. + 3\left[\frac{1}{3}(\rho_n - \rho_p)_{T_z=-3/2} + \frac{1}{3}(\delta\rho_{-3/2} + \delta\rho_{-1/2})\right]\right\} \\
&= -\frac{1}{6}\int_0^\infty dr 4\pi r^2 S_1^{\rm (CSB)}(\rho)[(\delta\rho_{3/2} - \delta\rho_{-3/2}) + (\delta\rho_{1/2} - \delta\rho_{-1/2})] \\
&= -\frac{1}{6}\int_0^\infty dr 4\pi r^2 S_1^{\rm (CSB)}(\rho)\left[(\delta\rho_{3/2} - \delta\rho_{-3/2}) + \frac{1}{3}(\delta\rho_{3/2} - \delta\rho_{-3/2})\right] \\
&= -\frac{8\pi}{9}\int_0^\infty dr r^2 S_1^{\rm (CSB)}(\rho)[(\delta\rho_{3/2} - \delta\rho_{-3/2})].
\end{aligned} \tag{A9}$$

$$\begin{aligned}
4d_2 &= \frac{1}{2}\left[3a_{\rm sym,2}^{\rm (CIB)}\left(A, \frac{3}{2}\right) - 3a_{\rm sym,2}^{\rm (CIB)}\left(A, -\frac{3}{2}\right) - a_{\rm sym,2}^{\rm (CIB)}\left(A, \frac{1}{2}\right) + a_{\rm sym,2}^{\rm (CIB)}\left(A, -\frac{1}{2}\right)\right] \\
&= \frac{A}{8}\left\{\frac{3}{\left(\frac{3}{2}\right)^2}\int_0^\infty 4\pi r^2 \frac{1}{\rho(r)} S_2^{\rm (CIB)}(\rho)(\rho_n - \rho_p)_{T_z=3/2}^2 dr - \frac{3}{\left(-\frac{3}{2}\right)^2}\int_0^\infty 4\pi r^2 \frac{1}{\rho(r)} S_2^{\rm (CIB)}(\rho)(\rho_n - \rho_p)_{T_z=-3/2}^2 dr\right. \\
&\quad - \frac{1}{\left(\frac{1}{2}\right)^2}\int_0^\infty 4\pi r^2 \frac{1}{\rho(r)} S_2^{\rm (CIB)}(\rho)\left[\frac{1}{3}(\rho_n - \rho_p)_{T_z=3/2} + \frac{1}{3}(\delta\rho_{3/2} + \delta\rho_{1/2})\right]^2 dr \\
&\quad \left. + \frac{1}{\left(-\frac{1}{2}\right)^2}\int_0^\infty 4\pi r^2 \frac{1}{\rho(r)} S_2^{\rm (CIB)}(\rho)\left[\frac{1}{3}(\rho_n - \rho_p)_{T_z=-3/2} + \frac{1}{3}(\delta\rho_{-3/2} + \delta\rho_{-1/2})\right]^2 dr\right\} \\
&= \frac{A}{8}\int_0^\infty dr 4\pi r^2 \frac{1}{\rho(r)} S_2^{\rm (CIB)}(\rho)\cdot\left\{\frac{4}{3}(\rho_n - \rho_p)_{T_z=3/2}^2 - \frac{4}{3}(\rho_n - \rho_p)_{T_z=-3/2}^2\right. \\
&\quad \left. - 4\left[\frac{1}{3}(\rho_n - \rho_p)_{T_z=3/2} + \frac{1}{3}(\delta\rho_{3/2} + \delta\rho_{1/2})\right]^2 + 4\left[\frac{1}{3}(\rho_n - \rho_p)_{T_z=-3/2} + \frac{1}{3}(\delta\rho_{-3/2} + \delta\rho_{-1/2})\right]^2\right\} \\
&= \frac{A}{8}\int_0^\infty dr 4\pi r^2 \frac{1}{\rho(r)} S_2^{\rm (CIB)}(\rho)\cdot\left\{\frac{8}{9}(\rho_n - \rho_p)_{T_z=3/2}^2 - \frac{8}{9}(\rho_n - \rho_p)_{T_z=-3/2}^2\right. \\
&\quad \left. - \frac{4}{9}[(\delta\rho_{3/2} + \delta\rho_{1/2})^2 + 2(\rho_n - \rho_p)_{T_z=3/2}(\delta\rho_{3/2} + \delta\rho_{1/2})]\right.
\end{aligned}$$

$$
\begin{aligned}
&+\frac{4}{9}[(\delta\rho_{-3/2}+\delta\rho_{-1/2})^2+2(\rho_n-\rho_p)_{T_z=-3/2}(\delta\rho_{-3/2}+\delta\rho_{-1/2})]\Big\}\\
&=\frac{A}{8}\int_0^\infty dr4\pi r^2\frac{1}{\rho(r)}S_2^{(\mathrm{CIB})}(\rho)\cdot\Big\{\frac{8}{9}(\rho_n-\rho_p)^2_{T_z=3/2}-\frac{8}{9}(\rho_n-\rho_p)^2_{T_z=-3/2}-\frac{32}{27}\big(\delta\rho^2_{3/2}-\delta\rho^2_{-3/2}\big)\\
&+\frac{8}{9}\Big[(\rho_n-\rho_p)_{T_z=-3/2}\Big(\frac{5}{3}\delta\rho_{-3/2}+\frac{1}{3}\delta\rho_{3/2}\Big)-(\rho_n-\rho_p)_{T_z=3/2}\Big(\frac{5}{3}\delta\rho_{3/2}+\frac{1}{3}\delta\rho_{-3/2}\Big)\Big]\Big\}\\
&=\frac{A}{8}\int_0^\infty dr4\pi r^2\frac{1}{\rho(r)}S_2^{(\mathrm{CIB})}(\rho)\cdot\Big\{\frac{8}{9}[\delta\rho_{3/2}+\delta\rho_{-3/2}][(\rho_n-\rho_p)_{T_z=3/2}-(\rho_n-\rho_p)_{T_z=-3/2}]-\frac{32}{27}\big(\delta\rho^2_{3/2}-\delta\rho^2_{-3/2}\big)\\
&+\frac{8}{9}\Big[(\rho_n-\rho_p)_{T_z=-3/2}\Big(\frac{5}{3}\delta\rho_{-3/2}+\frac{1}{3}\delta\rho_{3/2}\Big)-(\rho_n-\rho_p)_{T_z=3/2}\Big(\frac{5}{3}\delta\rho_{3/2}+\frac{1}{3}\delta\rho_{-3/2}\Big)\Big]\Big\}\\
&=\frac{A}{8}\int_0^\infty dr4\pi r^2\frac{1}{\rho(r)}S_2^{(\mathrm{CIB})}(\rho)\Big\{-\frac{32}{27}\big(\delta\rho^2_{3/2}-\delta\rho^2_{-3/2}\big)-\frac{16}{27}(\delta\rho_{3/2}-\delta\rho_{-3/2})(\delta\rho_{3/2}+\delta\rho_{-3/2})\Big\}\\
&=-\frac{2A}{9}\int_0^\infty dr4\pi r^2\frac{1}{\rho(r)}S_2^{(\mathrm{CIB})}(\rho)\big(\delta\rho^2_{3/2}-\delta\rho^2_{-3/2}\big).
\end{aligned}
\tag{A10}
$$

Finally, the d coefficient for the $T=3/2$ isobaric quartets takes the form of

$$
d=2d_1+\frac{4d_2}{A}=-\frac{8\pi}{9}\int_0^\infty r^2S_1^{(\mathrm{CSB})}(\rho)(\delta\rho_{3/2}-\delta\rho_{-3/2})dr-\frac{8\pi}{9}\int_0^\infty r^2\frac{S_2^{(\mathrm{CIB})}(\rho)}{\rho(r)}\big(\delta\rho^2_{3/2}-\delta\rho^2_{-3/2}\big)dr. \tag{A11}
$$

For $T=2$ isobaric quintets, similarly, the $\rho_n-\rho_p$ is summarized as

$$
\rho_n-\rho_p=\begin{cases}(\rho_n-\rho_p)_{T_z=2}, & T_z=2\\ \frac{1}{2}(\rho_n-\rho_p)_{T_z=2}+\frac{1}{4}(\delta\rho_2+\delta\rho_1), & T_z=1\\ \delta\rho_0, & T_z=0\\ \frac{1}{2}(\rho_n-\rho_p)_{T_z=-2}+\frac{1}{4}(\delta\rho_{-2}+\delta\rho_{-1}), & T_z=-1\\ (\rho_n-\rho_p)_{T_z=-2}. & T_z=-2\end{cases}
$$

We expand the symmetry energy $a^{(\mathrm{CSB})}_{\mathrm{sym},1}(A,T_z)T_z$ and $a^{(\mathrm{CIB})}_{\mathrm{sym},2}(A,T_z)T_z^2$ as $a^{(\mathrm{CSB})}_{\mathrm{sym},1}(A,T_z)T_z=a_1+b_1T_z+c_1T_z^2+d_1T_z^3+e_1T_z^4$ and $a^{(\mathrm{CIB})}_{\mathrm{sym},2}(A,T_z)T_z^2=a_2+b_2T_z+c_2T_z^2+d_2T_z^3+e_2T_z^4$, and thus Eq. (2) is written as

$$
\begin{aligned}
\mathrm{ME}(A,T,T_z)&=a+(b_c+\Delta_{\mathrm{nH}})T_z+2\big(a_1+b_1T_z+c_1T_z^2+d_1T_z^3+e_1T_z^4\big)+c_cT_z^2+\frac{4}{A}\big(a_2+b_2T_z+c_2T_z^2+d_2T_z^3+e_2T_z^4\big),\\
&=\Big(a+2a_1+\frac{4a_2}{A}\Big)+\Big(b_c+\Delta_{\mathrm{nH}}+2b_1+\frac{4b_2}{A}\Big)T_z+\Big(c_c+2c_1+\frac{4c_2}{A}\Big)T_z^2+\Big(2d_1+\frac{4d_2}{A}\Big)T_z^3+\Big(2e_1+\frac{4e_2}{A}\Big)T_z^4.
\end{aligned}
\tag{A12}
$$

The GIMME for quintets is reduced as

$$
\mathrm{ME}(A,T,T_z)=a+bT_z+cT_z^2+dT_z^3+eT_z^4. \tag{A13}
$$

with

$$
d=2d_1+\frac{4d_2}{A}, \tag{A14}
$$

$$
e=2e_1+\frac{4e_2}{A}. \tag{A15}
$$

The d_1, d_2, e_1, e_2 coefficients are given by

$$
\begin{aligned}
2d_1&=\frac{1}{3}\big[a^{(\mathrm{CSB})}_{\mathrm{sym},1}(A,2)+a^{(\mathrm{CSB})}_{\mathrm{sym},1}(A,-2)-a^{(\mathrm{CSB})}_{\mathrm{sym},1}(A,1)-a^{(\mathrm{CSB})}_{\mathrm{sym},1}(A,-1)\big]\\
&=\frac{1}{12}\int_0^\infty 4\pi r^2S_1^{(\mathrm{CSB})}(\rho)(\rho_n-\rho_p)_{T_z=2}dr-\frac{1}{12}\int_0^\infty 4\pi r^2S_1^{(\mathrm{CSB})}(\rho)(\rho_n-\rho_p)_{T_z=-2}dr\\
&-\frac{1}{6}\int_0^\infty 4\pi r^2S_1^{(\mathrm{CSB})}(\rho)\Big[\frac{1}{2}(\rho_n-\rho_p)_{T_z=2}+\frac{1}{4}(\delta\rho_2+\delta\rho_1)\Big]dr
\end{aligned}
$$

$$
\begin{aligned}
&+\frac{1}{6}\int_0^\infty 4\pi r^2 S_1^{(\mathrm{CSB})}(\rho)\left[\frac{1}{2}(\rho_n-\rho_p)_{T_z=-2}+\frac{1}{4}(\delta\rho_{-2}+\delta\rho_{-1})\right]dr\\
&=\frac{1}{12}\int_0^\infty dr 4\pi r^2 S_1^{(\mathrm{CSB})}(\rho)\Big\{(\rho_n-\rho_p)_{T_z=2}-(\rho_n-\rho_p)_{T_z=-2}\\
&-2\left[\frac{1}{2}(\rho_n-\rho_p)_{T_z=2}+\frac{1}{4}(\delta\rho_2+\delta\rho_1)\right]+2\left[\frac{1}{2}(\rho_n-\rho_p)_{T_z=-2}+\frac{1}{4}(\delta\rho_{-2}+\delta\rho_{-1})\right]\Big\}\\
&=-\frac{1}{24}\int_0^\infty dr 4\pi r^2 S_1^{(\mathrm{CSB})}(\rho)[\delta\rho_2+\delta\rho_1-\delta\rho_{-2}-\delta\rho_{-1}]\\
&=-\frac{1}{24}\int_0^\infty dr 4\pi r^2 S_1^{(\mathrm{CSB})}(\rho)\left[\delta\rho_2-\delta\rho_{-2}+\frac{1}{2}(\delta\rho_2-\delta\rho_{-2})\right]\\
&=-\frac{\pi}{4}\int_0^\infty r^2 S_1^{(\mathrm{CSB})}(\rho)[\delta\rho_2-\delta\rho_{-2}]dr. \qquad \text{(A16)}
\end{aligned}
$$

$$
\begin{aligned}
12e_1 &= a_{\mathrm{sym},1}^{(\mathrm{CSB})}(A,2)-a_{\mathrm{sym},1}^{(\mathrm{CSB})}(A,-2)-2a_{\mathrm{sym},1}^{(\mathrm{CSB})}(A,1)+2a_{\mathrm{sym},1}^{(\mathrm{CSB})}(A,-1)+3a_{\mathrm{sym},1}^{(\mathrm{CSB})}(A,T_z)T_z|_{T_z=0}\\
&=\frac{1}{4}\int_0^\infty 4\pi r^2 S_1^{(\mathrm{CSB})}(\rho)(\rho_n-\rho_p)_{T_z=2}dr+\frac{1}{4}\int_0^\infty 4\pi r^2 S_1^{(\mathrm{CSB})}(\rho)(\rho_n-\rho_p)_{T_z=-2}dr\\
&-\int_0^\infty 4\pi r^2 S_1^{(\mathrm{CSB})}(\rho)\left[\frac{1}{2}(\rho_n-\rho_p)_{T_z=2}+\frac{1}{4}(\delta\rho_2+\delta\rho_1)\right]dr\\
&-\int_0^\infty 4\pi r^2 S_1^{(\mathrm{CSB})}(\rho)\left[\frac{1}{2}(\rho_n-\rho_p)_{T_z=-2}+\frac{1}{4}(\delta\rho_{-2}+\delta\rho_{-1})\right]dr+3\frac{1}{2T_z}T_z|_{T_z=0}\int_0^\infty 4\pi r^2 S_1^{(\mathrm{CSB})}(\rho)\delta\rho_0 dr\\
&=\frac{1}{4}\int_0^\infty dr 4\pi r^2 S_1^{(\mathrm{CSB})}(\rho)\{(\rho_n-\rho_p)_{T_z=2}+(\rho_n-\rho_p)_{T_z=-2}\\
&-[2(\rho_n-\rho_p)_{T_z=2}+(\delta\rho_2+\delta\rho_1)]-[2(\rho_n-\rho_p)_{T_z=-2}+(\delta\rho_{-2}+\delta\rho_{-1})]+6\delta\rho_0\}\\
&=-\pi\int_0^\infty dr r^2 S_1^{(\mathrm{CSB})}(\rho)\{[(\rho_n-\rho_p)_{T_z=2}+(\delta\rho_2+\delta\rho_1)]+[(\rho_n-\rho_p)_{T_z=-2}+(\delta\rho_{-2}+\delta\rho_{-1})]-6\delta\rho_0\}\\
&=-\pi\int_0^\infty dr r^2 S_1^{(\mathrm{CSB})}(\rho)\{[(\rho_n-\rho_p)_{T_z=2}+(\rho_n-\rho_p)_{T_z=-2}]+[(\delta\rho_2+\delta\rho_1)+(\delta\rho_{-2}+\delta\rho_{-1})]-6\delta\rho_0\}\\
&=-\pi\int_0^\infty dr r^2 S_1^{(\mathrm{CSB})}(\rho)[(\delta\rho_2+\delta\rho_{-2})+(\delta\rho_2+\delta\rho_1)+(\delta\rho_{-2}+\delta\rho_{-1})-6\delta\rho_0]\\
&=0. \qquad \text{(A17)}
\end{aligned}
$$

$$
\begin{aligned}
6d_2 &= 2a_{\mathrm{sym},2}^{(\mathrm{CIB})}(A,2)-2a_{\mathrm{sym},2}^{(\mathrm{CIB})}(A,-2)-a_{\mathrm{sym},2}^{(\mathrm{CIB})}(A,1)+a_{\mathrm{sym},2}^{(\mathrm{CIB})}(A,-1)\\
&=\frac{A}{4}\left\{\frac{2}{4}\int_0^\infty 4\pi r^2\frac{1}{\rho(r)}S_2^{(\mathrm{CIB})}(\rho)(\rho_n-\rho_p)_{T_z=2}^2dr-\frac{2}{4}\int_0^\infty 4\pi r^2\frac{1}{\rho(r)}S_2^{(\mathrm{CIB})}(\rho)(\rho_n-\rho_p)_{T_z=-2}^2dr\right.\\
&-\int_0^\infty 4\pi r^2\frac{1}{\rho(r)}S_2^{(\mathrm{CIB})}(\rho)\left[\frac{1}{2}(\rho_n-\rho_p)_{T_z=2}+\frac{1}{4}(\delta\rho_2+\delta\rho_1)\right]^2dr\\
&\left.+\int_0^\infty 4\pi r^2\frac{1}{\rho(r)}S_2^{(\mathrm{CIB})}(\rho)\left[\frac{1}{2}(\rho_n-\rho_p)_{T_z=-2}+\frac{1}{4}(\delta\rho_{-2}+\delta\rho_{-1})\right]^2dr\right\}\\
&=\frac{A}{4}\int_0^\infty dr 4\pi r^2\frac{1}{\rho(r)}S_2^{(\mathrm{CIB})}(\rho)\cdot\left\{\frac{1}{2}(\rho_n-\rho_p)_{T_z=2}^2-\frac{1}{2}(\rho_n-\rho_p)_{T_z=-2}^2\right.\\
&\left.-\left[\frac{1}{2}(\rho_n-\rho_p)_{T_z=2}+\frac{1}{4}(\delta\rho_2+\delta\rho_1)\right]^2+\left[\frac{1}{2}(\rho_n-\rho_p)_{T_z=-2}+\frac{1}{4}(\delta\rho_{-2}+\delta\rho_{-1})\right]^2\right\}\\
&=\frac{A}{16}\int_0^\infty dr 4\pi r^2\frac{1}{\rho(r)}S_2^{(\mathrm{CIB})}(\rho)\Big\{\left[(\rho_n-\rho_p)_{T_z=2}^2-(\rho_n-\rho_p)_{T_z=-2}^2\right]\\
&-\frac{1}{4}[(\delta\rho_2+\delta\rho_1)^2-(\delta\rho_{-2}+\delta\rho_{-1})^2]-(\rho_n-\rho_p)_{T_z=2}(\delta\rho_2+\delta\rho_1)+(\rho_n-\rho_p)_{T_z=-2}(\delta\rho_{-2}+\delta\rho_{-1})\Big\}\\
&=\frac{A}{16}\int_0^\infty dr 4\pi r^2\frac{1}{\rho(r)}S_2^{(\mathrm{CIB})}(\rho)\left\{-\frac{3}{4}\left(\delta\rho_2^2-\delta\rho_{-2}^2\right)-\frac{3}{4}(\delta\rho_2+\delta\rho_{-2})(\delta\rho_2-\delta\rho_{-2})\right\}
\end{aligned}
$$

$$= \frac{A}{16}\int_0^\infty dr 4\pi r^2 \frac{1}{\rho(r)} S_2^{(\mathrm{CIB})}(\rho)\left\{-\frac{3}{2}\left(\delta\rho_2^2 - \delta\rho_{-2}^2\right)\right\}$$
$$= -\frac{3A}{32}\int_0^\infty dr 4\pi r^2 \frac{1}{\rho(r)} S_2^{(\mathrm{CIB})}(\rho)\left(\delta\rho_2^2 - \delta\rho_{-2}^2\right). \tag{A18}$$

$$6e_2 = a_{\mathrm{sym},2}^{(\mathrm{CIB})}(A,2) + a_{\mathrm{sym},2}^{(\mathrm{CIB})}(A,-2) - a_{\mathrm{sym},2}^{(\mathrm{CIB})}(A,1) - a_{\mathrm{sym},2}^{(\mathrm{CIB})}(A,-1) + \frac{3}{2}a_{\mathrm{sym},2}^{(\mathrm{CIB})}(A,T_z)T_z^2\big|_{T_z=0}$$
$$= \frac{A}{4}\left\{\frac{1}{4}\int_0^\infty 4\pi r^2 \frac{1}{\rho(r)} S_2^{(\mathrm{CIB})}(\rho)(\rho_n-\rho_p)_{T_z=2}^2 dr + \frac{1}{4}\int_0^\infty 4\pi r^2 \frac{1}{\rho(r)} S_2^{(\mathrm{CIB})}(\rho)(\rho_n-\rho_p)_{T_z=-2}^2 dr\right.$$
$$- \int_0^\infty \frac{4\pi r^2}{\rho(r)} S_2^{(\mathrm{CIB})}(\rho)\left[\frac{1}{2}(\rho_n-\rho_p)_{T_z=2} + \frac{1}{4}(\delta\rho_2+\delta\rho_1)\right]^2 dr$$
$$\left.- \int_0^\infty \frac{4\pi r^2}{\rho(r)} S_2^{(\mathrm{CIB})}(\rho)\left[\frac{1}{2}(\rho_n-\rho_p)_{T_z=-2} + \frac{1}{4}(\delta\rho_{-2}+\delta\rho_{-1})\right]^2 dr + \frac{3}{2T_z^2}T_z^2\big|_{T_z=0}\int_0^\infty 4\pi r^2 \frac{1}{\rho(r)} S_2^{(\mathrm{CIB})}(\rho)\delta\rho_0^2 dr\right\}$$
$$= \frac{A}{16}\int_0^\infty dr 4\pi r^2 \frac{1}{\rho(r)} S_2^{(\mathrm{CIB})}(\rho)\cdot\left\{(\rho_n-\rho_p)_{T_z=2}^2 + (\rho_n-\rho_p)_{T_z=-2}^2\right.$$
$$\left.-\left[(\rho_n-\rho_p)_{T_z=2} + \frac{1}{2}(\delta\rho_2+\delta\rho_1)\right]^2 - \left[(\rho_n-\rho_p)_{T_z=-2} + \frac{1}{2}(\delta\rho_{-2}+\delta\rho_{-1})\right]^2 + 6\delta\rho_0^2\right\}$$
$$= -\frac{A}{16}\int_0^\infty dr 4\pi r^2 \frac{1}{\rho(r)} S_2^{(\mathrm{CIB})}(\rho)\cdot\left\{\frac{1}{4}(\delta\rho_2+\delta\rho_1)^2 + (\rho_n-\rho_p)_{T_z=2}(\delta\rho_2+\delta\rho_1)\right.$$
$$\left.+\frac{1}{4}(\delta\rho_{-2}+\delta\rho_{-1})^2 + (\rho_n-\rho_p)_{T_z=-2}(\delta\rho_{-2}+\delta\rho_{-1}) - 6\delta\rho_0^2\right\}$$
$$= -\frac{A}{64}\int_0^\infty dr 4\pi r^2 \frac{1}{\rho(r)} S_2^{(\mathrm{CIB})}(\rho)\cdot\left\{\left(2\delta\rho_2 - \frac{\delta\rho_2-\delta\rho_{-2}}{4}\right)^2 + 4(\rho_n-\rho_p)_{T_z=2}\left(2\delta\rho_2 - \frac{\delta\rho_2-\delta\rho_{-2}}{4}\right)\right.$$
$$\left.+\left(2\delta\rho_{-2} + \frac{\delta\rho_2-\delta\rho_{-2}}{4}\right)^2 + 4(\rho_n-\rho_p)_{T_z=-2}\left(2\delta\rho_{-2} + \frac{\delta\rho_2-\delta\rho_{-2}}{4}\right) - 24\delta\rho_0^2\right\}$$
$$= -\frac{A}{64}\int_0^\infty dr 4\pi r^2 \frac{1}{\rho(r)} S_2^{(\mathrm{CIB})}(\rho)\cdot\left\{\left(\frac{25}{8}\delta\rho_2^2 + \frac{25}{8}\delta\rho_{-2}^2 + \frac{7}{4}\delta\rho_2\delta\rho_{-2}\right)\right.$$
$$\left.+4(\rho_n-\rho_p)_{T_z=2}\left[(\delta\rho_2+\delta\rho_{-2}) + \frac{3}{4}(\delta\rho_2-\delta\rho_{-2})\right] + 4(\rho_n-\rho_p)_{T_z=-2}\left[(\delta\rho_2+\delta\rho_{-2}) - \frac{3}{4}(\delta\rho_2-\delta\rho_{-2})\right] - 24\delta\rho_0^2\right\}$$
$$= -\frac{3A}{64}\int_0^\infty dr 4\pi r^2 \frac{1}{\rho(r)} S_2^{(\mathrm{CIB})}(\rho)\left\{\frac{3}{8}(\delta\rho_2-\delta\rho_{-2})^2 + (\delta\rho_2-\delta\rho_{-2})[(\rho_n-\rho_p)_{T_z=2} - (\rho_n-\rho_p)_{T_z=-2}]\right\}. \tag{A19}$$

Finally, we obtain the d, e coefficients for the $T=2$ quintets taking the form of

$$d = 2d_1 + \frac{4d_2}{A}$$
$$= -\frac{\pi}{4}\int_0^\infty r^2 S_1^{(\mathrm{CSB})}(\rho)(\delta\rho_2-\delta\rho_{-2})dr - \frac{\pi}{4}\int_0^\infty \frac{r^2}{\rho(r)} S_2^{(\mathrm{CIB})}(\rho)\left(\delta\rho_2^2-\delta\rho_{-2}^2\right)dr, \tag{A20}$$
$$e = 2e_1 + \frac{4e_2}{A}$$
$$= -\frac{\pi}{64}\int_0^\infty dr \frac{r^2}{\rho(r)} S_2^{(\mathrm{CIB})}(\rho)(\delta\rho_2-\delta\rho_{-2})\cdot\left[11(\delta\rho_2-\delta\rho_{-2}) + 8\left(\rho_n^{\mathrm{exc}}|_{T_z=2} + \rho_p^{\mathrm{exc}}|_{T_z=-2}\right)\right], \tag{A21}$$

where $\rho_n^{\mathrm{exc}}|_{T_z=2}$ ($\rho_p^{\mathrm{exc}}|_{T_z=-2}$) is the density of the $|N-Z|$ excess neutrons (protons) in the $T_z=T$ ($T_z=-T$) nucleus.

[1] W. E. Heisenberg, Z. Phys. **77**, 1 (1932).
[2] E. P. Wigner, *in Proceedings of the R. A. Welch Foundation Conference on Chemical Research, Houston*, edited by W. O. Millikan (R. A. Welch Foundation, Houston, 1957), Vol. 1.
[3] S. Weinberg and S. B. Treiman, Phys. Rev. **116**, 465 (1959).
[4] W. Benenson and E. Kashy, Rev. Mod. Phys. **51**, 527 (1979).
[5] W. J. Huang, G. Audi, M. Wang, F. G. Kondev, S. Naimi, and X. Xu, Chin. Phys. C **41**, 030002 (2017).
[6] E. Kashy, W. Benenson, D. Mueller, and R. G. H. Robertson, Phys. Rev. C **11**, 1959 (1975).
[7] Y. H. Zhang, H. S. Xu, Y. A. Litvinov, X. L. Tu, X. L. Yan, S. Typel, K. Blaum, M. Wang, X. H. Zhou, Y. Sun, B. A. Brown, Y. J. Yuan, J. W. Xia, J. C. Yang, G. Audi, X. C. Chen, G. B. Jia, Z. G. Hu, X. W. Ma, R. S. Mao, B. Mei, P. Shuai, Z. Y. Sun, S. T. Wang, G. Q. Xiao, X. Xu, T. Yamaguchi, Y. Yamaguchi, Y. D. Zang, H. W. Zhao, T. C. Zhao, W. Zhang, and W. L. Zhan, Phys. Rev. Lett. **109**, 102501 (2012).
[8] A. T. Gallant, M. Brodeur, C. Andreoiu, A. Bader, A. Chaudhuri, U. Chowdhury, A. Grossheim, R. Klawitter, A. A. Kwiatkowski, K. G. Leach, A. Lennarz, T. D. Macdonald, B. E. Schultz, J. Lassen, H. Heggen, S. Raeder, A. Teigelhofer, B. A. Brown, A. Magilligan, J. D. Holt, J. Menendez, J. Simonis, A. Schwenk, and J. Dilling, Phys. Rev. Lett. **113**, 082501 (2014).
[9] Y. H. Lam *et al.*, At. Data Nucl. Data Tables **99**, 680 (2013).
[10] M. A. Bentley and S. M. Lenzi, Prog. Part. Nucl. Phys. **59**, 497 (2007).
[11] M. MacCormick and G. Audi, Nucl. Phys. A **925**, 61 (2014).
[12] M. Brodeur, T. Brunner, S. Ettenauer, A. Lapierre, R. Ringle, B. A. Brown, D. Lunney, and J. Dilling, Phys. Rev. Lett. **108**, 212501 (2012).
[13] A. Signoracci and B. A. Brown, Phys. Rev. C **84**, 031301(R) (2011).
[14] E. M. Henley and C. E. Lacy, Phys. Rev. **184**, 1228 (1969).
[15] G. Bertsch and S. Kahana, Phys. Lett. B **33**, 193 (1970).
[16] W. E. Ormand and B. A. Brown, Nucl. Phys. A **491**, 1 (1989).
[17] A. P. Zuker, S. M. Lenzi, G. Martinez-Pinedo, and A. Poves, Phys. Rev. Lett. **89**, 142502 (2002).
[18] K. Kaneko, Y. Sun, T. Mizusaki, and S. Tazaki, Phys. Rev. Lett. **110**, 172505 (2013).
[19] Y. H. Lam, N. A. Smirnova, and E. Caurier, Phys. Rev. C **87**, 054304 (2013).
[20] K. Kaneko, Y. Sun, T. Mizusaki, and S. Tazaki, Phys. Rev. C **89**, 031302(R) (2014).
[21] J. M. Dong, Y. H. Zhang, W. Zuo, J. Z. Gu, L. J. Wang, and Y. Sun, Phys. Rev. C **97**, 021301(R) (2018).
[22] N. Auerbach and A. Lev, Nucl. Phys. A **180**, 651 (1972).
[23] J. Britz, A. Pape, and M. S. Antony, At. Data Nucl. Data Tables **69**, 125 (1998).
[24] C. Y. Fu, Y. H. Zhang, X. H. Zhou, M. Wang, Y. A. Litvinov, K. Blaum, H. S. Xu, X. Xu, P. Shuai, Y. H. Lam, R. J. Chen, X. L. Yan, T. Bao, X. C. Chen, H. Chen, J. J. He, S. Kubono, D. W. Liu, R. S. Mao, X. W. Ma, M. Z. Sun, X. L. Tu, Y. M. Xing, P. Zhang, Q. Zeng, X. Zhou, W. L. Zhan, S. Litvinov, G. Audi, T. Uesaka, Y. Yamaguchi, T. Yamaguchi, A. Ozawa, B. H. Sun, Y. Sun, and F. R. Xu, Phys. Rev. C **98**, 014315 (2018).
[25] A. Kankainen, L. Canete, T. Eronen, J. Hakala, A. Jokinen, J. Koponen, I. D. Moore, D. Nesterenko, J. Reinikainen, S. Rinta-Antila, A. Voss, and J. Aysto, Phys. Rev. C **93**, 041304(R) (2016).
[26] M. B. Bennett, C. Wrede, B. A. Brown, S. N. Liddick, D. Perez-Loureiro, D. W. Bardayan, A. A. Chen, K. A. Chipps, C. Fry, B. E. Glassman, C. Langer, N. R. Larson, E. I. McNeice, Z. Meisel, W. Ong, P. D. OMalley, S. D. Pain, C. J. Prokop, S. B. Schwartz, S. Suchyta, P. Thompson, M. Walters, and X. Xu, Phys. Rev. C **93**, 064310(R) (2016).
[27] F. Herfurth, J. Dilling, A. Kellerbauer, G. Audi, D. Beck, G. Bollen, H. J. Kluge, D. Lunney, R. B. Moore, C. Scheidenberger, S. Schwarz, G. Sikler, and J. Szerypo (Isolde Collaboration), Phys. Rev. Lett. **87**, 142501 (2001).
[28] M. C. Pyle, A. Garcia, E. Tatar, J. Cox, B. K. Nayak, S. Triambak, B. Laughman, A. Komives, L. O. Lamm, J. E. Rolon, T. Finnessy, L. D. Knutson, and P. A. Voytas, Phys. Rev. Lett. **88**, 122501 (2002).
[29] C. Yazidjian, G. Audi, D. Beck, K. Blaum, S. George, C. Guenaut, F. Herfurth, A. Herlert, A. Kellerbauer, H. J. Kluge, D. Lunney, and L. Schweikhard, Phys. Rev. C **76**, 024308 (2007).
[30] R. Ringle, T. Sun, G. Bollen, D. Davies, M. Facina, J. Huikari, E. Kwan, D. J. Morrissey, A. Prinke, J. Savory, P. Schury, S. Schwarz, and C. S. Sumithrarachchi, Phys. Rev. C **75**, 055503 (2007).
[31] J. Su *et al.*, Phys. Lett. B **756**, 323 (2016).
[32] E. Chabanat, P. Bonche, P. Haensel, J. Meyer, and R. Schaeffer, Nucl. Phys. A **635**, 231 (1998).
[33] J. Dong, W. Zuo, and J. Gu, Phys. Rev. C **91**, 034315 (2015).
[34] B. A. Brown and R. Sherr, Nucl. Phys. A **322**, 61 (1979).
[35] M. Honma, T. Otsuka, B. A. Brown, and T. Mizusaki, Phys. Rev. C **65**, 061301(R) (2002).
[36] M. Honma, T. Otsuka, B. A. Brown, and T. Mizusaki, Phys. Rev. C **69**, 034335 (2004).
[37] E. Epelbaum, H.-W. Hammer, and U.-G. Meißner, Rev. Mod. Phys. **81**, 1773 (2009).
[38] B. E. Glassman, D. Perez-Loureiro, C. Wrede, J. Allen, D. W. Bardayan, M. B. Bennett, B. A. Brown, K. A. Chipps, M. Febbraro, C. Fry, M. R. Hall, O. Hall, S. N. Liddick, P. OMalley, W. Ong, S. D. Pain, S. B. Schwartz, P. Shidling, H. Sims, P. Thompson, and H. Zhang, Phys. Rev. C **92**, 042501(R) (2015).
[39] E. G. Adelberger, C. Ortiz, A. Garcia, H. E. Swanson, M. Beck, O. Tengblad, M. J. G. Borge, I. Martel, and H. Bichsel (ISOLDE Collaboration), Phys. Rev. Lett. **83**, 1299 (1999); **83**, 3101 (1999).
[40] K. Blaum, G. Audi, D. Beck, G. Bollen, F. Herfurth, A. Kellerbauer, H. J. Kluge, E. Sauvan, and S. Schwarz, Phys. Rev. Lett. **91**, 260801 (2003).
[41] S. Triambak, A. Garcia, E. G. Adelberger, G. J. P. Hodges, D. Melconian, H. E. Swanson, S. A. Hoedl, S. K. L. Sjue, A. L. Sallaska, and H. Iwamoto, Phys. Rev. C **73**, 054313 (2006).
[42] A. A. Kwiatkowski, B. R. Barquest, G. Bollen, C. M. Campbell, D. L. Lincoln, D. J. Morrissey, G. K. Pang, A. M. Prinke, J. Savory, S. Schwarz, C. M. Folden, D. Melconian, S. K. L. Sjue, and M. Block, Phys. Rev. C **80**, 051302(R) (2009).
[43] A. Kankainen, T. Eronen, D. Gorelov, J. Hakala, A. Jokinen, V. S. Kolhinen, M. Reponen, J. Rissanen, A. Saastamoinen, V. Sonnenschein, and J. Aysto, Phys. Rev. C **82**, 052501(R) (2010).
[44] N. Auerbach, Phys. Rep. **98**, 273 (1983).
[45] N. Auerbach and N. V. Giai, Phys. Rev. C **24**, 782 (1981).